MOLECULAR ENDOCRINOLOGY

The Osteogenic Transcription Factor Runx2 Controls Genes Involved in Sterol/Steroid Metabolism, Including Cyp11a1 in Osteoblasts

Nadiya M. Teplyuk, Ying Zhang, Yang Lou, John R. Hawse, Mohammad Q. Hassan, Viktor I. Teplyuk, Jitesh Pratap, Mario Galindo, Janet L. Stein, Gary S. Stein, Jane B. Lian and Andre J. van Wijnen

Mol. Endocrinol. 2009 23:849-861 originally published online Apr 2, 2009; , doi: 10.1210/me.2008-0270

The Osteogenic Transcription Factor Runx2 Controls Genes Involved in Sterol/Steroid Metabolism, Including Cyp11a1 in Osteoblasts

Nadiya M. Teplyuk, Ying Zhang, Yang Lou, John R. Hawse, Mohammad Q. Hassan, Viktor I. Teplyuk, Jitesh Pratap, Mario Galindo, Janet L. Stein, Gary S. Stein, Jane B. Lian, and Andre J. van Wijnen

Department of Cell Biology and Cancer Center (N.M.T., Y.Z., Y.L., M.Q.H., J.P., J.L.S., G.S.S., J.B.L., A.J.v.W.), and Bioinformatics Core (V.I.T.), Program in Molecular Medicine, University of Massachusetts Medical School, Worcester, Massachusetts 01655; Department of Biochemistry and Molecular Biology (J.R.H.), Mayo Clinic College of Medicine, Rochester, Minnesota 55905; and Program of Cellular and Molecular Biology (M.G.), Institute of Biomedical Sciences, Faculty of Medicine, University of Chile, 70061 Santiago, Chile

Steroid hormones including (1,25)-dihydroxyvitamin D3, estrogens, and glucocorticoids control bone development and homeostasis. We show here that the osteogenic transcription factor Runx2 controls genes involved in sterol/steroid metabolism, including Cyp11a1, Cyp39a1, Cyp51, Lss, and Dhcr7 in murine osteoprogenitor cells. Cyp11a1 (P450scc) encodes an approximately 55-kDa mitochondrial enzyme that catalyzes side-chain cleavage of cholesterol and is rate limiting for steroid hormone biosynthesis. Runx2 is coexpressed with Cyp11a1 in osteoblasts as well as nonosseous cell types (*e.g.* testis and breast cancer cells), suggesting a broad biological role for Runx2 in sterol/steroid metabolism. Notably, osteoblasts and breast cancer cells express an approximately 32-kDa truncated isoform of Cyp11a1 that is nonmitochondrial and localized in both the cytoplasm and the nucleus. Chromatin immunoprecipitation analyses and gel shift assays show that Runx2 binds to the Cyp11a1 gene promoter in osteoblasts, indicating that Cyp11a1 is a direct target of Runx2. Specific Cyp11a1 knockdown with short hairpin RNA increases cell proliferation, indicating that Cyp11a1 normally suppresses osteoblast proliferation. We conclude that Runx2 regulates enzymes involved in sterol/steroid-related metabolic pathways and that activation of Cyp11a1 by Runx2 may contribute to attenuation of osteoblast growth. **(*Molecular Endocrinology* 23: 849–861, 2009)**

Steroid hormones are key regulators of bone development and homeostasis (1–10). Systemic deficiency of steroids by mutations in their cognate steroid hormone receptors [*e.g.* for (1,25)-dihydroxyvitamin D3, androgen, and estrogen] or steroid metabolism (*e.g.* Cyp19 aromatase) decreases mineralization, increases bone resorption, and/or inhibits growth plate closure (5, 11–15). Chronic therapeutic administration of glucocorticoids (3, 16) or natural reductions in steroid hormone levels (17–21) cause osteoporosis by impairing the metabolic balance of osteoblasts and bone-resorbing osteoclasts (22–26). Steroid hormones are prominently produced in selected nonosseous tissues, but enzymes involved in steroid hormone synthesis and breakdown are endogenously expressed in osteoblasts and may locally metabolize steroid precursors into potent steroid receptor agonists (27–29).

Expression of many steroid hormone-responsive genes in osteoblasts is regulated by the Runt-related transcription factor Runx2/Cbfa1 (6, 30–35), which is essential for osteoblast maturation (36–38). In addition, steroid hormones including 1,25 $(OH)_2$-vitamin D3 and estrogen modulate the expression of Runx2 at the transcriptional level (39, 40). Furthermore, the *trans*-activation function of Runx2 is modulated in part by steroid-related posttranslational mechanisms (41, 42). Other examples of genetic and gene regulatory interplay between Runx2 and steroid hormones (*e.g.* glucocorticoids and estrogens) are also evident (43, 44).

ISSN Print 0888-8809 ISSN Online 1944-9917
Printed in U.S.A.

doi: 10.1210/me.2008-0270 Received August 1, 2008. Accepted March 16, 2009.
First Published Online April 2, 2009

Abbreviations: aa, Amino acid; CMV, cytomegalovirus; DAPI, 4′,6-diamidino-2-phenylindole; FBS, fetal bovine serum; GFP, green fluorescent protein; PBSA, PBS containing 0.5% BSA; qPCR, quantitative PCR; shRNA, short hairpin RNA.

The potent osteogenic activity of Runx2 is linked to its principal function as an epigenetic regulator of phenotype commitment and cell growth (45–49). Loss of Runx2 deregulates normal osteoblast growth (47–50), whereas forced expression of Runx2 suppresses proliferation of osteoblasts (48, 51) and nonbone cells (52), consistent with its proposed general role as a gene related to cancer (53). To accommodate its role as a regulator of osteoblast proliferation, the levels of Runx2 oscillate during the cell cycle and are highest in G1 (48, 54). Multiple Runx2 target genes have been identified that contribute to osteogenic or proliferation-related functions of Runx2 (51, 55–58), but our understanding of Runx2-responsive genes remains incomplete.

In this study, we examined whether Runx2 is capable of controlling genes involved in steroid hormone signaling or metabolism. We identified a panel of genes encoding enzymes that control sterol metabolism. One of these genes (Cyp11a1) is upregulated during osteoblast differentiation and expresses a unique short Cyp11a1 isoform that, unlike the full-length protein, is not concentrated into mitochondria. Short hairpin RNA (shRNA) knockdown of this isoform increases osteoblast proliferation, suggesting Cyp11a1 contributes to Runx2-mediated attenuation of cell growth.

Results

Identification of Runx2 target genes related to sterol metabolism

To address whether the biological interrelationships between Runx2 and steroid hormones are reflected by direct regulatory pathways, we examined whether Runx2 is capable of controlling the expression of genes related to steroid hormone metabolism. We have previously used immortalized mouse calvaria osteoprogenitors derived from Runx2-null mice as a cell culture model (59) to identify Runx2 target genes during recapitulation of a developmental transition when proliferating mesenchymal stem cells become osteoprogenitors and exhibit Runx2-attenuated cell growth (51). Gene expression profiling was used to assess which genes respond to the introduction of Runx2, a transcriptionally inert deletion mutant (Runx2Δ361) or a green fluorescent protein (GFP)-expressing empty vector into Runx2-null cells. Duplicate RNA samples were harvested from adenovirus Runx2 infected cells at 24 h after induction of Runx2 gene expression and hybridized to Affymetrix mouse cDNA arrays (Mouse Genome 430 2.0 Array). Statistical analysis of the data set revealed that a series of genes involved in sterol metabolism is coordinately controlled by Runx2, along with known Runx2 target genes (Table 1 and Fig. 1).

We tested a representative subset of six genes using quantitative PCR (qPCR) analysis for responsiveness to Runx2 expression (Fig. 2) in parallel with a prototypical Runx2 target gene (osteocalcin) as positive control and GAPDH as negative control. Our results validate Runx2-dependent expression for five of these six genes (*i.e.* P450 cytochrome proteins Cyp11a1, Cyp39A1, and Cyp51 as well as Lss and Dhcr7). Thus, Runx2 modulates a number of genes linked to sterol/steroid metabolism through direct or indirect mechanisms.

Modulation of Cyp11a1 gene expression by Runx2 in committed osteoblasts

The most prominently modulated sterol-related gene in our Affymetrix analysis encodes the cholesterol side-cleaving enzyme Cyp11a1 (60, 61). Cyp11a1 protein expression is normally below the level of detection in osteoprogenitors that do not express Runx2. However, Cyp11a1 mRNA expression is dramatically induced within 24 h after introduction of Runx2 protein into Runx2-null cells as determined by Affymetrix expression analysis (Table 1) and qPCR analysis (Fig. 2). To assess whether Runx2 can up-regulate Cyp11a1 in committed osteoblasts, we performed semiquantitative PCR analysis. We analyzed RNA samples from mouse Runx2-null osteoprogenitors, mouse MC3T3 osteoblasts, and SV40 transformed human O4T8 osteoblasts infected with wild-type Runx2 and the corresponding empty adenoviral vector (Fig. 3). The forced expression of Runx2 rapidly induces Cyp11a1 expression (Fig. 3). Exogenous Runx2 also stimulates osteocalcin and osteopontin expression but does not alter GAPDH or 18S rRNA levels (Fig. 3). Thus, Runx2 selectively regulates expression of the Cyp11a1 gene.

To assess whether CYP11A1 up-regulation by Runx2 is dose dependent, we transfected Runx2-null cells and MC3T3 cells with different amounts of a cytomegalovirus (CMV)-based expression vector encoding Runx2. Runx2-null osteoprogenitors and immature MC3T3 osteoblasts have very low levels of endogenous Cyp11a1, but Cyp11a1 mRNA levels increase in proportion to the amount of exogenous Runx2 gene induction (data not shown; see also Fig. 5B below). Taken together, Runx2 is a key rate-limiting factor for Cyp11a1 gene expression in both preosteoblastic progenitors and committed osteoblasts.

Cyp11a1 gene expression is induced during osteoblastic differentiation

We further investigated the physiological relevance of Cyp11A1 induction by Runx2 by characterizing endogenous expression of Cyp11a1 during MC3T3 osteoblastic differentiation in relation to endogenous Runx2 levels and other osteoblast marker genes (Fig. 4A). There is a significant elevation of Cyp11a1 gene expression throughout the MC3T3 differentiation time course, along with osteocalcin (Fig. 4A) and other osteoblastic markers (*e.g.* osteopontin and alkaline phosphatase; data not shown). The data show that Cyp11a1 is expressed at maximal levels in mature osteoblasts in parallel with the Runx2-dependent expression of the osteocalcin. Hence, Cyp11a1 is physiologically expressed in differentiated bone cells that express Runx2.

We also investigated Cyp11a1 expression in Runx2-null progenitor cells that were reconstituted with wild-type Runx2 and stimulated to differentiate into the osteoblastic lineage in the presence of osteogenic medium (Fig. 4B). The combination of exogenous Runx2 and osteogenic conditions induces alkaline phosphatase expression (Fig. 4B), and is known to restore the ability of Runx2-null cells to differen-

TABLE 1. Runx2 regulates a panel of genes related to sterol/steroid hormone synthesis, metabolism and signaling in osteoblasts

Gene symbol	Gene name	Runx2 WT *vs.* GFP	WT *vs.* Δ361
Enzymes involved in sterol metabolism			
Cyp11a1	Cytochrome P450, family 11, subfamily a, polypeptide 1	4.2	3.9
Lss	Lanosterol synthase	3.1	2.7
Dhcr7	7-Dehydrocholesterol reductase	2.3	2.3
Cyp39a1	Cytochrome P450, family 39, subfamily a, polypeptide 1	2.3	2.7
Hsd3b7	Hydroxy-δ-5-steroid dehydrogenase, 3β- and steroid δ-isomerase 7	1.7	1.5
Fdps	Farnesyl diphosphate synthetase	1.6	1.7
Sult2b1	Sulfotransferase family, cytosolic, 2B, member 1	1.6	1.4
Hsd17b7	Hydroxysteroid (17-β) dehydrogenase 7	1.5	
Fdxr	Ferredoxin reductase	1.5	1.7
Cyp51	Cytochrome P450, family 51		1.6
Sc5d	Sterol C5 desaturase		1.5
Ch25 h	Cholesterol 25-hydroxylase		−2.4
Cyp1b1	Cytochrome P450, family 1, subfamily b, polypeptide 1	−3.0	−2.3
Por	Cytochrome P450 oxidoreductase		−1.6
Cyp20a1	Cytochrome P450, family 20, subfamily a, polypeptide 1	−1.7	−1.5
Kinases and gene regulators involved in sterol metabolism			
Stat5a	Signal transducer and activator of transcription 5A	2.0	1.7
Pbx1	Pre B-cell leukemia transcription factor 1	−1.8	
Prkaa1	Protein kinase, AMP-activated, α1 catalytic subunit	−1.8	
Transporters, binding proteins and receptors involved in sterol metabolism			
Abca2	ATP-binding cassette, subfamily A (ABC1), member 2	1.7	1.6
Ebpl	Emopamil binding protein-like	1.6	
Gig1	Glucocorticoid induced gene 1	−2.2	−1.5
Nr3c1	Nuclear receptor subfamily 3, group c, member 1	−2.0	−1.7
Abca1	ATP-binding cassette, subfamily A (ABC1), member 1	−1.9	−1.8
Plekhh2	Pleckstrin homology domain containing, family H, member 2	−1.7	
Ldlr	Low density lipoprotein receptor	−1.6	−1.6
Osbpl2	Oxysterol binding protein-like 2	−1.6	−1.6
Osbpl3	Oxysterol binding protein-like 3	−1.6	−1.5
Osbpl9	Oxysterol binding protein-like 9	−1.5	
Osbpl8	Oxysterol binding protein-like 8	−1.4	
Hdlbp	High-density lipoprotein binding protein	−1.5	
Known Runx2 target genes			
Spp1	Secreted phosphoprotein 1 (osteopontin)	13.6	23.1
Bglap1	Bone γ carboxyglutamate protein 2 (osteocalcin)	6.3	7.7
Mmp13	Matrix metalloproteinase 13	7.8	6.1

Selected genes exhibit a statistically significant increase or decrease in expression 24 h after the infection based on Student's *t* test ($P < 0.05$). The data are presented as a fold change in the expression signal between cells expressing Runx2 wild type (WT) *vs.* Δ361 mutant or Runx2 WT *vs.* GFP. The cluster of steroid signaling- and metabolism-related genes was extracted by functional annotation clustering of Affymetrix data in the David 2.0 web-based environment (Database for Annotation, Visualization and Integrated Discovery, http://david.abcc.ncifcrf.gov/).

tiate and express other mature osteoblastic markers (59). Importantly, the presence of Runx2 clearly stimulates Cyp11a1 gene expression, and this effect becomes more pronounced as differentiation progresses. Thus, Runx2 is rate limiting for Cyp11a1 gene expression during differentiation along the osteoblastic lineage.

We analyzed expression of Runx2, Runx1, and Cyp11a1 by qPCR analysis of total cellular RNA from a panel of osseous and reproductive tissues. Cyp11a1 mRNA levels are low but detectable in calvaria and tibia, where Runx2 is expressed at very high levels (Fig. 4D). High levels of Cyp11a1 mRNA expression as well as Runx1 and Runx2 are observed in mature ovary and

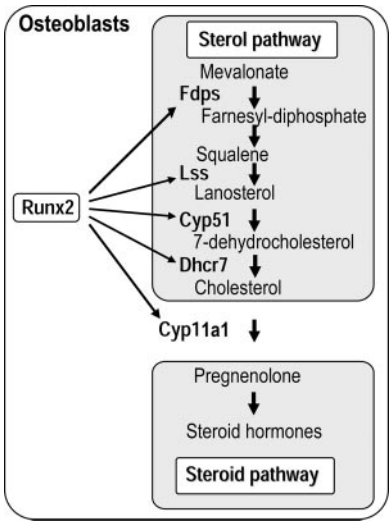

FIG. 1. The schematic representation of the multiple consecutive enzymatic reactions that are required for the biosynthesis of cholesterol (sterol pathway) and its conversion to pregnenolone (steroid pathway). Our data show that several key enzymes of cholesterol biosynthesis and metabolism are expressed in osteoblasts, and their expression is induced by the bone-specific transcription factor Runx2.

testis (Fig. 4D), corroborating previous reports showing robust Runx1-dependent expression of Cyp11a1 in granulosa cells and periovulatory follicles in rat and mouse (62, 63). Interestingly, during fetal development or postnatal testicular development, total Runx levels correlate with Cyp11a1 expression (data not shown). Taken together, Runx2 and Runx1 may both regulate Cyp11a1 during development in osseous and reproductive tissues.

Runx2 induces a small isoform of Cyp11a1 in osteoblasts

We performed Western blot analysis to assess whether the increase in Cyp11a1 mRNA expression that we observed translates into a corresponding induction of Cyp11a1 protein levels. As expected, forced expression of wild-type Runx2 but not Δ361 results in robust levels of Cyp11a1 protein (Fig. 5A). Expression of Cyp11a1 is proportional to the amount of Runx2 expression, indicating that Runx2 titrates Cyp11a1 protein levels (Fig. 5B), consistent with a direct effect of Runx2 on Cyp11a1 gene transcription (see below). Interestingly, lysates

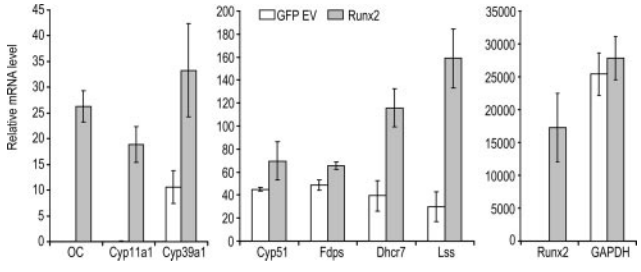

FIG. 2. Validation of Runx2-responsive expression of genes related to sterol/steroid pathways by qPCR analysis. Real-time qPCR analysis was used to validate mRNA expression levels of a subset of genes that depend on Runx2 as identified by Affymetrix analysis (see Table 1). Osteocalcin levels were measured to establish the inducibility of a representative Runx2-responsive gene. Expression values for all genes were plotted relative to each other and normalized using GAPDH as internal control. *Error bars* represent SE of qPCR data for three independent experiments.

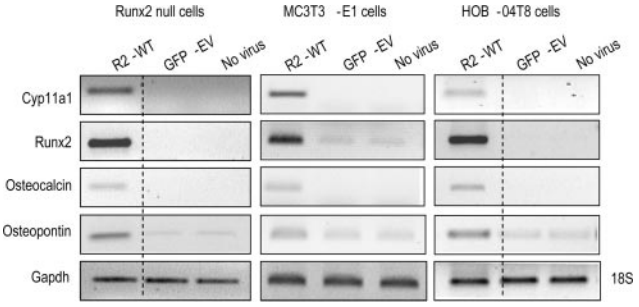

FIG. 3. Runx2 induces Cyp11a1 expression in mouse and human osteoblasts. Representative semiquantitative RT-PCR analysis was performed to examine stimulation of Cyp11a1 by Runx2 in mouse MC3T3 or human HOB-04T8 osteoblasts compared with Runx2-null cells. Levels for Runx2, osteocalcin, osteopontin, and GAPDH (or 18S) gene transcripts were assessed in parallel. RNA samples were prepared 24 h after infection with adenoviral vectors that express wild-type Runx2 or GFP. GAPDH and 18S RNA were used as internal controls for, respectively, mouse and human samples. RT-PCR products were subjected to electrophoresis in 2% agarose gels and visualized by ethidium bromide staining. Digital images were inverted to display black bands on a white background. *Dashed lines* indicate noncontiguous lanes on the same gel.

from testis or prostate tissues yield the expected approximately 55-kDa Cyp11a1 protein, whereas osteoblasts and Runx2-null osteoprogenitors express primarily an approximately 32-kDa species upon induction by Runx2 (Fig. 5C). Breast cancer-derived MDA-MB-231 cells express both the 55- and 32-kDa isoforms (Fig. 5C). Although the 55-kDa isoform of Cyp11a1 is normally localized in mitochondria (64, 65), the N-terminally truncated form of human CYP11A1 (isoform B) lacks the N-terminal mitochondrial localization signal (66) (GenBank accession no. NM_001099773 and NP_0010933). Thus, the short murine Cyp11a1 isoform that is induced by Runx2 may not be localized in mitochondria (see below).

Expression of the 32-kDa isoform of human Cyp11a1 is regulated by alternative splicing and utilization of an internal translational start codon. We examined the distribution of exons present in mouse Cyp11a1 mRNA using RT-qPCR (Fig. 6). Cyp11a1 mRNA is clearly expressed endogenously in testis and upon induction by Runx2 in MC3T3 osteoblasts and Runx2-null osteoprogenitors. More importantly, exons encoding the first and second ATG start codon of the mouse Cyp11a1 mRNA are detected at comparable abundance in all three RNA samples (Fig. 6), suggesting that each sample expresses a full-length Cyp11a1 mRNA. It appears that the murine 32-kDa isoform of Cyp11a1 is not produced by omission of the first ATG-containing exon (as is the case for human CYP11A1) but perhaps by alternative translational initiation.

Cyp11a1 gene is directly regulated by Runx2 at the promoter level

Forced expression data clearly indicate that Cyp11a1 gene expression is responsive to modulations in the levels of Runx2 (Figs. 2–4). To investigate whether Runx2 can directly control Cyp11a1 gene transcription, we first tested whether the induction of endogenous Cyp11a1 expression requires the DNA binding and *trans*-activation functions of Runx2 upon introduction into Runx2-null cells (Fig. 7A). The data show that Cyp11a1 is robustly up-regulated by wild-type Runx2 but not when its C-terminal *trans*-activation domain is deleted (Runx2

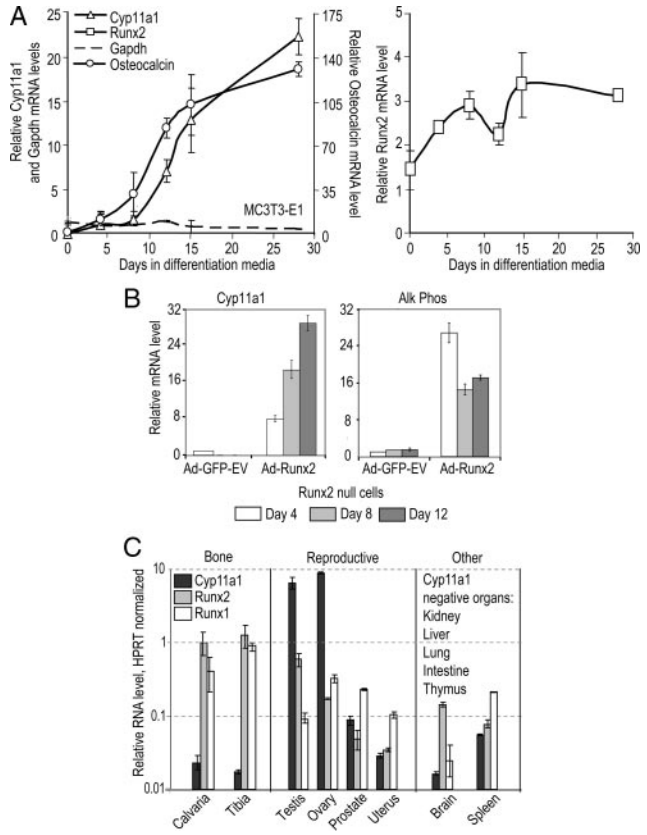

FIG. 4. Runx2-dependent expression of Cyp11a1 during osteoblast maturation. A, Expression levels of Cyp11a1, Runx2, and osteocalcin RNA levels were analyzed by qPCR during osteoblast differentiation. Confluent MC3T3 cells were induced to differentiate with ascorbic acid and β-glycerophosphate for 28 d. Expression values were normalized based on GAPDH mRNA levels. *Error bars* represent SE of two independent experiments. B, Expression levels of Cyp11a1 and alkaline phosphatase mRNAs were determined by qPCR in Runx2-null cells in the presence or absence of exogenous Runx2. Runx2-null cells were infected with adenovirus expressing Runx2 (Ad-Runx2) or GFP empty vector (Ad-GFP-EV), and differentiation media was added to cells 24 h after infection. Samples were prepared at 4-d intervals and analyzed as described in A. C, Levels of Cyp11a1 mRNA in relation to Runx2 and Runx1 mRNAs were determined by qPCR analysis in adult mouse tissues (2 months of age). Levels of gene expression were normalized relative to HPRT mRNA. *Error bars* represent the SD of duplicate qPCR of a representative experiment.

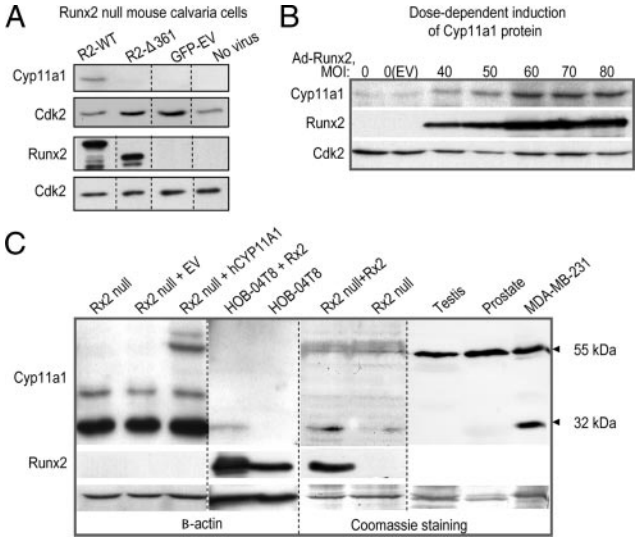

FIG. 5. Runx2 induces a small Cyp11a1 protein isoform in Runx2-null cells. A, Western blot analysis shows expression of Cyp11a1 protein in Runx2-null cells infected (for 36 h) with an adenovirus vector expressing wild-type (WT) Runx2 but not the Runx2 Δ361 mutant or GFP as indicated. CDK2 protein was used as an internal control. *Dashed lines* reflect digital juxtaposition of parallel lanes from the same gel. The Cyp11a1 species we detected has a molecular mass of about 32 kDa (see C). B, Dose-dependent stimulation of Cyp11a1 protein expression is evident in lysates from Runx2-null cells infected (for 36 h) with the indicated amounts of an adenoviral vector expression wild-type Runx2 protein. Cyp11a1 and Runx2 levels were detected by Western blot analysis, whereas CDK2 protein levels were used as an internal control. C, Different Cyp11a1 protein isoforms are expressed in different cell types and tissues. The full-length approximately 55-kDa Cyp11a1 protein isoform is expressed in testis and prostate tissues as well as MDA-MB-231 breast cancer cells but not in Runx2-null cells. Runx2-null cells and HOB-04T8 cells reconstituted with wild-type Runx2 and MDA-MB-231 cells (that are known to express Runx2 ectopically due to the transformed state of the cells) each express a short approximately 32-kDa isoform. The low-mobility bands (>55 kDa) in the *left* lane are not induced by Runx2 and considered nonspecific. When exogenously expressed in Runx2-null cells, CYP11A1 gives an approximately 55-kDa band, confirming the antibodies' specificity (labeled Rx2 null + hCYP11A1).

mutants Δ432 and Δ361) or when its DNA-binding domain (mutant DBDM) is mutated (Fig. 7A). Hence, transcriptional activation by Runx2 is critical for induction of Cyp11a1.

Both the mouse and human Cyp11a1 gene promoters contain at least five Runx2 consensus motifs, although their locations within the respective 5′-flanking regions are not strictly conserved (Fig. 7B). We performed EMSAs to examine whether these sites can support Runx2 binding *in vitro*. To permit a quantitative comparison of relative binding strengths for each of these sites, we performed competition analyses using unlabeled oligos spanning the Runx2 motifs and a known probe that encompasses a classical Runx2 binding site in the rat osteocalcin gene (site C or OSE2). Nuclear extracts from rat ROS17/2.8 osteosarcoma cells were used in binding reactions, because these cells are known to express high endogenous levels of Runx2 and were used to define site C/OSE2 in previous studies (35–37). The EMSA results show that one motif (Cyp3, nucleotides −1005 to −999) is an effective competitor, and three motifs are moderately effective competitors (Cyp2, Cyp4, and Cyp5) (Fig. 7, C and D). The most upstream motif we tested (Cyp1) did not compete for Runx2 binding to the established Runx2 element site C (Fig. 7, C and D). Thus, we have empirically validated that there is at least one high-affinity Runx2 site in the mouse Cyp11a1 gene promoter and that three additional sites may contribute to transcriptional control of the Cyp11a1 gene.

We next performed transient transfection assays with Cyp11a1 promoter fragments fused to the luciferase promoter. For luciferase reporters, we selected a promoter fragment spanning about 1.4 kb of 5′ sequence that contains the four validated Runx2 motifs, including the high-affinity Runx2 element (Cyp 3) (Fig. 8A). Coexpression of Runx2 clearly enhances reporter gene activity of the −1.4-kb Cyp11A gene promoter by about 3- to 4-fold (Fig. 8A). However, Runx2 does not activate the −0.3-kb Cyp 11A gene promoter that lacks three Runx2 motifs (Cyp2, Cyp 3, and Cyp4), or the −0.2-kb promoter that does not contain any discernable Runx2 motifs (Fig. 8A). We note that the single Runx2 site in the −0.3-kb promoter is not sufficient for Runx2-mediated transcriptional stimulation. The transfection data indicate that Runx2 directly activates Cyp11a1 transcription and that this activation requires cognate sites between −1.4 and −0.3 kb.

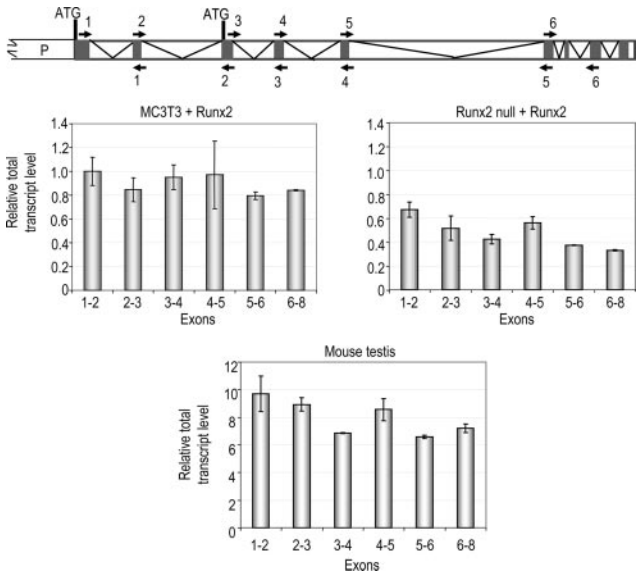

FIG. 6. The full-length transcript of Cyp11a1 gene is induced by Runx2 in osteoblasts. To determine whether the short osteoblast-specific isoform of Cyp11a1 protein can be generated by alternative transcription or alternative splicing in mouse, six different pairs of primers for mouse Cyp11a1 gene were designed spanning the first eight of nine different exons of the gene. qPCR was performed with the total cDNA synthesized from the random hexamer primers to measure different Cyp11a1 exons representation in Cyp11a1 transcript induced by Runx2 in mouse calvaria Runx2-null cells and MC3T3 cells and in the native transcript from the mouse testis. All pairs of primers amplified comparable levels of products, indicating that all of the first eight exons of mouse Cyp11a1 gene are present at the same amount after induction of gene expression by Runx2 in osteoblasts. The endogenous (noninduced) level of Cyp11a1-specific RNA was significantly (around 500-fold) lower then Runx2-induced transcript in this experiment, possibly minimally contributing to the reaction (data not shown).

To provide further *in vivo* evidence that Cyp11a1 is a direct Runx2 target, we analyzed Runx2 interactions with the Cyp11a1 promoter by chromatin immunoprecipitation analysis. Runx2-null cells do not exhibit Runx2 binding to the Cyp11a1 promoter above background levels (Fig. 8B). Robust interactions are observed throughout the promoter when Runx2 is reintroduced by adenoviral infection (Fig. 8B). Chromatin immunoprecipitates prepared using an IgG antibody exhibit signals at or below background levels. We conclude that Cyp11a1 is a Runx2-responsive gene and may represent an integral component of a biological program that is controlled by Runx2 to regulate enzymes mediating sterol/steroid metabolism.

The 32-kDa isoform of Cyp11a1 is not localized in mitochondria

Forced expression of Runx2 in Runx2-null cells induces a 32-kDa isoform of Cyp11a1 that is shorter than the full-length 55-kDa isoform that is localized in part in mitochondria (see Fig. 5). To assess the subcellular localization of the 32-kDa isoform, we performed immunofluorescence microscopy analysis using a Cyp11a1 antibody and find that the localization of Cyp11a1 varies between MC3T3 osteoblasts and Runx2-null cells (Fig. 9A). In most MC3T3 cells (85%), we observe diffuse cytoplasmic/nuclear staining, although perinuclear tubular (12%) or vesicular (3%) staining patterns are also detected. In Runx2-null cells, the majority of cells exhibit perinuclear tubular staining (80%) or diffuse cytoplasmic/nuclear staining (19%) and rarely cytoplasmic vesicular staining (1%). The specificity of Cyp11a1 antibodies is indicated by recognition of exogenously expressed flag and GFP-tagged Cyp11a1 proteins (see supplemental Fig. S1, published as supplemental data on The Endocrine Society's Journals Online web site at http://mend.endojournals.org). Therefore, similar to the full-length 55-kDa Cyp11a1 protein, the majority of the 32-kDa protein variant is expressed in the cytoplasm.

The 55-kDa Cyp11a1 protein is a full-length isoform of 526 amino acids (aa). The 32-kDa short isoform is predicted to be generated by alternative translation at an internal ATG to yield a 371-aa protein that is analogous to human CYP11A1 isoform B. We investigated the subcellular localization of the 371-aa isoform relative to the full-length 526-aa isoform using the exogenous expression of either Flag epitope-tagged proteins (Fig. 9B) or GFP fusion proteins (Fig. 9C). Consistent with the data obtained using a Cyp11a1 antibody, we find that both short and long isoforms of Cyp11a1 are predominantly localized in the cytoplasm. However, the Flag-tagged 526-aa variant exhibits mostly a tubular pattern, whereas the 371-aa has a vesicular pattern. These results indicate that the two Cyp11a1 isoforms are localized in separate compartments.

We studied the subcellular localization of the long and short isoforms using MitoTracker dye, a cell-permeable probe that selectively labels mitochondria (Fig. 9D). The 526-aa isoform of Cyp11a1 clearly colocalizes with MitoTracker dye, albeit that there is also diffuse nonmitochondrial cytoplasmic staining for Cyp11a1 (Fig. 9D and data not shown). In contrast, the 32-kDa (371 aa) variant of Cyp11a1 does not colocalize with MitoTracker dye. Taken together, the short isoform of Cyp11a1 does not reside in mitochondria and may perform a novel cellular function.

shRNA knockdown of Cyp11a1 increases osteoblast proliferation

We studied the function of Cyp11a1 by shRNA-mediated depletion of its endogenous levels in Runx2-null cells or MC3T3 osteoblasts (Fig. 10). shRNA for Cyp11a1 decreases its mRNA levels with limited effects on the expression of other genes (Fig. 10A) and diminishes Cyp11a1 protein levels (Fig. 10B). In Runx2 null cells that do or do not express exogenous Runx2, knockdown of Cyp11a1 causes a statistically significant, albeit quantitatively modest, increase in cell growth (Fig. 10C). A comparable stimulatory effect on cell proliferation is observed upon knockdown of Cyp11a1 expressed endogenously in MC3T3 cells (Fig. 10D). Thus, consistent with the cell growth-suppressive potential of Runx2, its target Cyp11a1 may support attenuation of cell proliferation.

Discussion

Runx2 is known to control a number of phenotypic genes that are coregulated by steroid hormone receptors (31, 32, 67), as well as genes for steroid receptors (68). In this study, we show that Runx2 controls a series of genes encoding enzymes involved

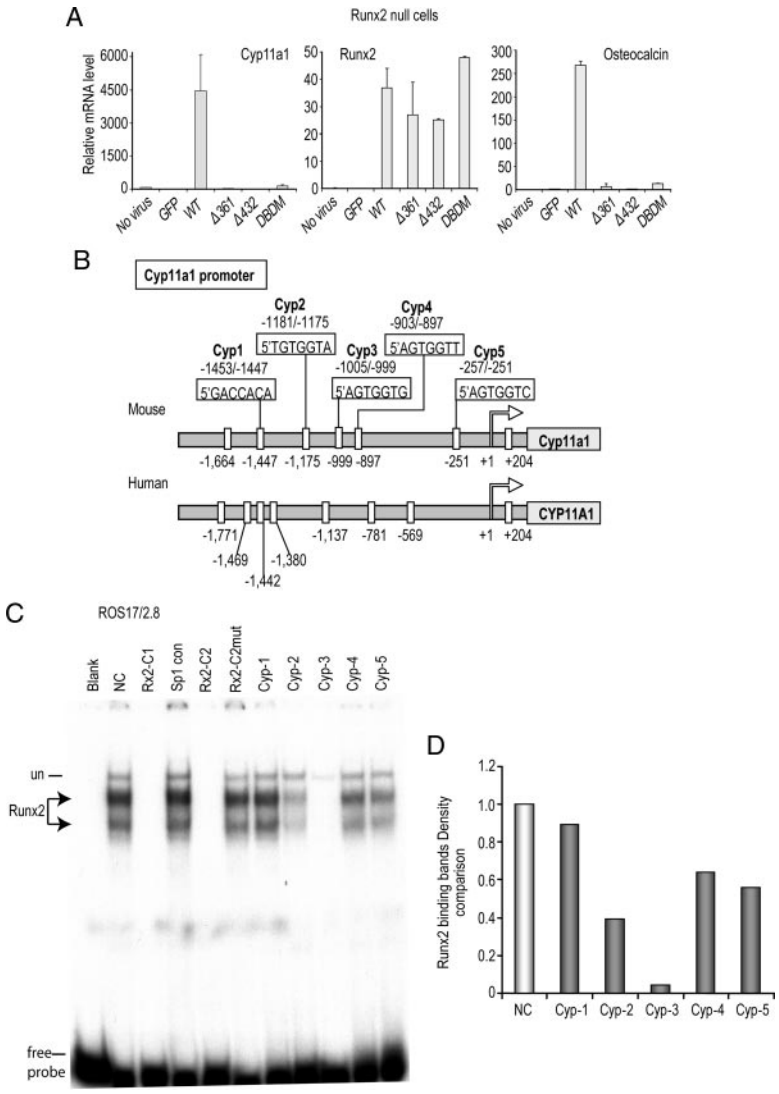

FIG. 7. Transcriptional activation of Cyp11a1 involves promoter recognition by Runx2 protein. A, Cyp11a1 expression is activated by forced expression of wild-type Runx2 protein but not mutant Runx2 proteins with defects in *trans*-activation (*i.e.* C-terminal deletion mutants Δ361 and Δ432) or DNA binding (DBDM). RNA samples were obtained from cells infected for 40 h with adenoviral vectors expressing the indicated Runx2 proteins. The mRNA levels of Cyp11a1, Runx2, and osteocalcin were analyzed by qPCR and normalized using GAPDH as internal control. *Error bars* indicate SD of two independent experiments. B, Human and mouse CYP11A1 gene promoters were analyzed for the presence of Runx2 binding consensus sites (5′-HGYGGT-3′). C, Runx2 binding to cognate motifs in the mouse Cyp11a1 gene promoter was determined by EMSAs using a radiolabeled probe spanning a classical Runx2 element (site C or OSE2; oligonucleotide Rx2-C1). Binding reactions were prepared using protein samples prepared from ROS17/2.8 cells that contain high levels of Runx2 protein. Competition assays were performed by adding 100-fold molar excess of unlabeled oligonucleotides to the binding reaction. The following competitor oligonucleotides were used: Rx2-C1 (self-competition), Sp1 consensus (Sp1 con), Rx2-C2 (Runx2 motif in the rat Runx2 gene) (79), a corresponding mutant oligo in which the Runx2 motif is mutated (Rx2-C2 mut), and five oligonucleotides that span putative Runx2 motifs in the Cyp11a1 promoter (respectively, Cyp-1, -2, -3, -4, and -5). Protein-DNA complexes were visualized by autoradiography of a 6% acrylamide gel (un, unrelated complex). D, Quantitation of the Runx2-DNA complexes presented in C.

in sterol and steroid metabolism. Cyp11a1, a representative sterol/steroid-related gene, is directly regulated by Runx2 in osteoblasts through Runx2 elements in the Cyp11a1 promoter. The finding that Runx2 controls expression of sterol-related genes indicates that Runx2 may locally modulate sterol and steroid compounds within the osteoblast microenvironment. The biological relevance of these modulations is reflected by the importance of cholesterol metabolism in osteoblasts and bone homeostasis (69).

Our observation that Cyp11a1 is a Runx2 target gene complements previous studies that have shown that Cyp11a1 and Runx1 are coregulated and that Cyp11a1 is Runx1 responsive in ovulating follicles (62, 63). Interestingly, data presented here and in other studies (70) indicate that Runx2 is also highly expressed in testis, a reproductive tissue in which Cyp11a1 is also abundantly expressed. Hence, the Cyp11a1 gene may perhaps be regulated by any of the three Runx transcription factors, depending on the cell type and tissue context in which specific Runx members are expressed. We consider it less likely, nevertheless, that Cyp11a1 induction by Runx2 may have a systemic endocrine effect. Cyp11a1 null mice die within the first 2 d after birth and survive slightly longer than Runx2-null mouse pups. Both Runx2 and Cyp11a1 null mice exhibit severe growth retardation. However, unlike Cyp11a1 knockout mice, Runx2-null mice do not develop muscular atrophy and gonadal defects (71), indicating that Runx2 deficiency does not have dominant effects on circulating hormone levels. Based on the inhibitory effects of Cyp11a1 in immature osteoblasts and the prominent expression of Cyp11a1 in late-stage osteoblasts, we propose that Runx2 control of Cyp11a1 supports metabolic functions in both proliferating and postproliferative bone cells (*i.e.* mature osteoblasts and/or mineral-embedded osteocytes).

The full-length Cyp11a1 protein (~55 kDa) is localized in mitochondria. Immunoblotting experiments show that Runx2 up-regulates a short isoform (~32 kDa) of Cyp11a1 that is localized in both the cytoplasm and the nucleus but not in mitochondria. Alternative mRNA splicing is known to generate a short (~32 kDa) isoform in human cells, because the human CYP11A1 gene contains an alternative 5′ exon that eliminates the normal ATG, whereas an internal methionine codon functions as an alternative ATG start codon. Although this alternative exon is conserved in the primate lineage, it appears to be absent in the rodent lineage. The truncated mouse Cyp11a1 isoform may be generated without alternative splicing in mouse cells by alternative translational initiation (by preferred recognition of the internal ATG) and/or posttranslational cleavage.

Because we observe that a subset of the short 32-kDa isoform of Cyp11a1 localizes in the nucleus (supplemental Fig. S2), the possibility arises that the function of Cyp11a1 in mature osteoblasts may be related to metabolism of sterol and steroid compounds inside the nucleus. Recent data suggest that Cyp11a1 can hydroxylate vitamin D2 and vitamin D3 (72–74). At least some of these vitamin D metabolites have

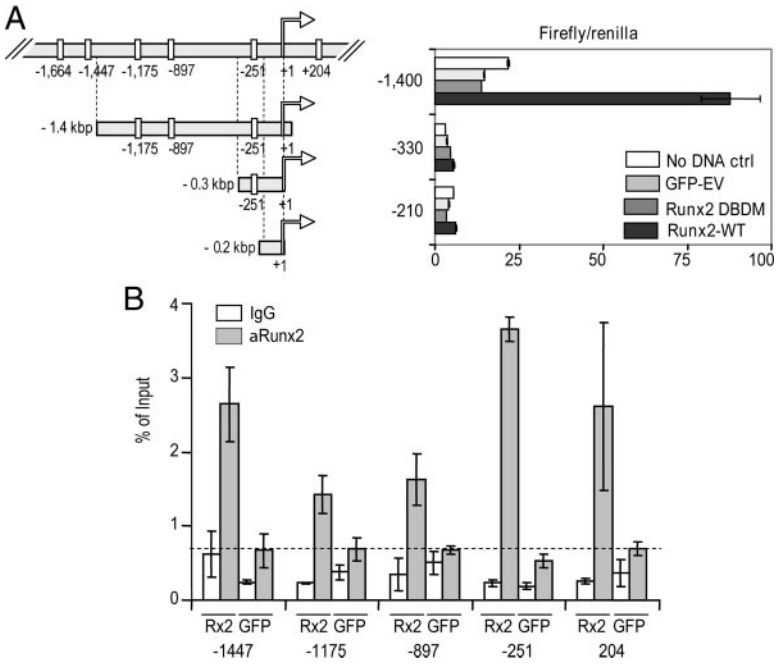

FIG. 8. Runx2 directly regulates the mouse Cyp11a1 promoter. A, Runx2 activates the Cyp11a1 promoter and requires a promoter fragment spanning three Runx2 motifs. Luciferase reporter constructs fused to different Cyp11a1 promoter fragments with different endpoints (*i.e.* 1.4 kb, 330 bp, and 210 bp) were transfected into Runx2-null cells that express wild-type Runx2, a Runx2 DNA-binding domain mutant, or GFP (negative control). Relative firefly luciferase values were normalized using renilla luciferase. *Error bars* represent the standard error of representative experiments performed in duplicate. B, Chromatin immunoprecipitation analysis shows that Runx2 binds to multiple sites in the endogenous Cyp11a1 promoter. Runx2 or GFP was expressed in Runx2-null cells upon adenoviral infection, and Runx2 binding to the promoter was assessed by qPCR analysis of immunoprecipitates obtained with Runx2 antibody (a Runx2) or nonspecific IgG. *Error bars* indicate the SD between duplicate samples of a representative experiment.

antiproliferative activities (*e.g.* reflected by reduced DNA synthesis). Thus, intranuclear production of biologically active vitamin D compounds by Cyp11a1 may support the antiproliferative properties of Runx2 in osteoblasts. Indeed, we observed a modest increase in cell proliferation after specific shRNA knockdown of Cyp11a1 expression, suggesting that induction of Cyp11a1 expression by Runx2 functionally contributes to Runx2-dependent attenuation of osteoblast proliferation.

Materials and Methods

Tissue culture and mouse tissues

MC3T3-E1 and Runx2-null cells were grown in αMEM from GIBCO/Invitrogen (Grand Island, NY), catalog item 11900-024. U2OS human osteosarcoma cells were cultured in McCoy's 5A medium (HyClone Laboratories, Inc., Logan, UT), ROS 17/2.8 cells were cultured in Ham's F12 medium (HyClone), and HEK293T cells were cultured in DMEM/high-glucose medium (HyClone). All cell types were maintained at 37 C and 5% CO_2 humidified atmosphere. Runx2-null cells are calvarial osteoprogenitor cells derived from Runx2 knockout mice that were generated by stable mouse telomerase gene (mTERT) integration in our laboratory as described (59). HOB 04T8 cells represent T-antigen transformed, conditionally immortalized human osteoblast cells, which grow at a permissive temperature of 34 C) as described previously (75). HOB 04T8 osteoblasts were grown in DMEM-F12 medium (GIBCO/Invitrogen) at 34 C and 5% CO_2 humidified atmosphere.

Media for MC3T3, Runx2-null, U2OS, and HOB cells were supplemented with 10% fetal bovine serum (FBS) from Atlanta Biologicals (Lawrenceville, GA). The medium for ROS cells was supplemented with 5% FBS from HyClone. All media were also supplemented with 30 mM penicillin-streptomycin and 100 mM L-glutamine.

For analysis of *in vivo* gene expression, mouse tissues were collected in 2 ml Trizol reagent and sonicated for 10–30 sec, and RNA was extracted by standard protocols. All procedures involving the care and use of C57 mice were approved by the Animal Research Committee at the University of Massachusetts Medical School.

Gene delivery by transfections and infections

For transfections, MC3T3 and Runx2-null cells were plated in 100-mm plates at a density of 0.4×10^6 cells per plate or in six-well plates at a density of 8.3×10^4 cells per well. After 24 h, cells were transfected using Lipofectamine Plus reagents according to the manufacturer's protocol (Invitrogen, Carlsbad, CA). U2OS cells were plated at 6.7×10^4 cells per well in six-well plates and transfected after 24 h using Fugene 6 transfection reagent (Roche Diagnostics GmbH, Mannheim, Germany) according to the manufacturer's protocol. Cells were collected 36 h after transfection.

For adenoviral infections, Runx2-null or MC3T3 cells were plated in six-well plates (12.5×10^4 cells per well). After 24 h, cells were infected with a 100 multiplicity of infection (MOI) of each virus for Runx2-null cells and 400 MOI for MC3T3 cells in 600 μl medium complemented with 1% FBS for 4 h. Then 400 μl αMEM containing 1% FBS medium was added, and cells were incubated for an additional 10 h. HOB cells were plated in six-well plates (12.5×10^4 cells per well) and infected after 24 h with 25 MOI of each virus for 4 h in 400 μl DMEM-F12 medium supplemented with 1% FBS. Infection efficiency was monitored by an Independent Ribosomal Entry Site (IRES)-driven GFP signal.

For shRNA-mediated knockdown of Cyp11a1 expression, Runx2-null cells were plated in six-well plates (1×10^5 cells per well) and infected 24 h later with lentivirus expressing rodent Cyp11a1 or nonspecific shRNA. Briefly, cells were treated with 1.5 ml nonpurified virus supernatant from packaging cells (HEK293T) and 0.5 ml complete fresh αMEM per well with a final concentration of 8 μg/ml hexadimethrine bromide (Polybrene; Sigma-Aldrich, Inc., St. Louis, MO). Plates were centrifuged upon addition of the virus at $1460 \times g$ at 37 C for 1 h. Infection efficiency was monitored by GFP coexpression at 3 d after infection.

Expression constructs and viruses

A pCMV5-Runx2 expression vector was generated by cloning the mouse Runx2 cDNA (MASNS isoform) into pCMV5. The cDNA of full-length Runx2 and its deletion mutants 1-361 (ΔC) and 1-432 (Δ432) as well as point mutants R182Q (DNA binding domain mutant) and HTY426-8AAA (Smad interaction mutant) were each recloned into an adenoviral vector (AdenoVator TM; Qbiogene, Irvine, CA) from the corresponding pcDNA vectors. Viruses were generated according to manufacturer's protocol (Qbiogene) and purified using an adenovirus purification kit (Promega, Madison, WI).

Human CYP11A1 full-length cDNA in pCMV-SPORT6-expressing vector was purchased from Mammalian Genome Collection of the American Type Culture Collection (Manassas, VA).

A mouse Cyp11a1 cDNA (ENSMUSG 00000032323) was used to construct an expression vector for both full-length Cyp11a1 and an N-terminally truncated form (using a 5′-deletion starting from nucleotide 50 of exon 3). Both cDNA fragments were amplified by PCR from mouse testis cDNA with specific primers (Table 2). PCR products were inserted to TOPO TA PCR cloning vector (Invitrogen) and subsequently subcloned into the *Eco*RI restriction site of pCMV-tag2B vector to obtain Cyp11a1 proteins with an N-terminal Flag tag (Stratagene, La Jolla,

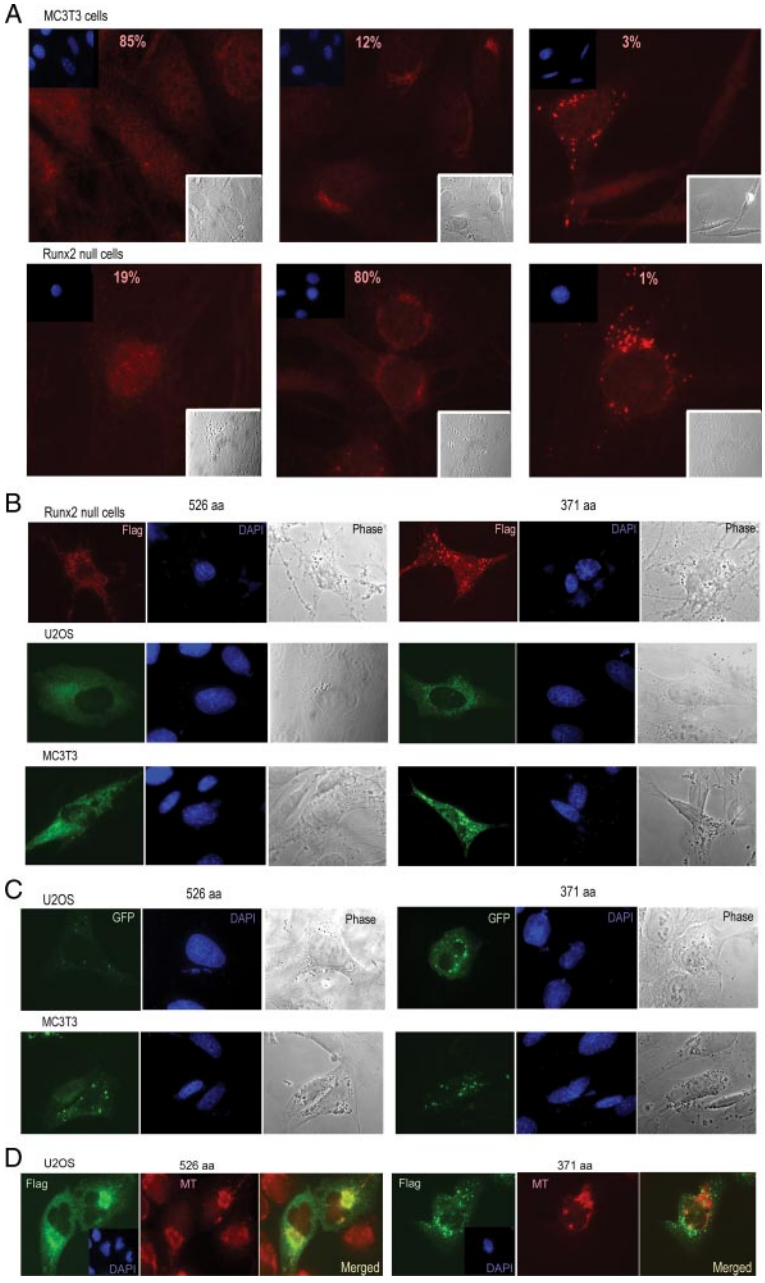

FIG. 9. Endogenous Cyp11a1 and the exogenous 371-aa isoform of Cyp11a1 exhibit similar intracellular localization in osteoblasts. A, Micrograph of endogenous Cyp11a1 protein present in Runx2-null osteoprogenitors and MC3T3 cells detected using *in situ* immunofluorescence. Cyp11a1 exhibits either punctuate perinuclear or weak nuclear staining in the majority of the cells. B, Intracellular localization of exogenously expressed Flag-Cyp11a1 fusion proteins in osteoblasts as detected with immunofluorescence staining of the Flag tag. Cells were transfected with either Flag-Cyp11a1-expressing constructs or empty vector control and then fixed and stained for the Flag-epitope and DAPI at 36 h after transfection. The full-length (526-aa) Cyp11a1 protein is localized in the cytoplasm as reflected by diffuse or tubular staining patterns. The truncated (371-aa) Cyp11a1 isoform has both nuclear and cytoplasmic localization and exhibits a more punctuate pattern. In some cells, Cyp11a1 foci are concentrated around the nucleus similarly to endogenous protein, whereas in other cells, they are distributed equally throughout cytoplasm. Cells transfected with the Flag-empty vector control did not have any detectable staining (data not shown). C, Intracellular localization of exogenously expressed N-terminal GFP-Cyp11a1 fusion proteins in osteoblasts. Cells were transfected with constructs expressing either full-length or truncated GFP-Cyp11a1 fusion proteins or control empty vector expressing GFP alone. Cells were fixed and stained for DAPI for visualization of the nucleus at 36 h after transfection. The intrinsic fluorescent signals of GFP fusion proteins were detected in these experiments. Both short and long isoforms of Cyp11a1 when fused to GFP have clear punctate cytoplasmic localization, with the short form concentrating mostly around the nucleus. D, Full-length (526 aa) but not truncated (371 aa) Cyp11a1 protein localizes to mitochondria. U2OS cells were transfected with Flag-Cyp11a1-expressing constructs. After 36 h, Mitotracker dye was added to the cells for 15 min, followed by fixing and staining of cells for the Flag tag and DAPI.

CA) or into pEGFP-C2 vector (Clontech, Mountain View, CA) to yield an N-terminal GFP tag. All constructs were sequences to validate the correct reading frame and absence of mutations.

Rodent Cyp11a1-specific shRNA-expressing lentiviral vectors (pGIPz) and nonsilencing RNA in pGIPz were purchased from Open Biosystems/Thermo Fisher Scientific (Huntsville, AL). Lentiviruses were packaged in HEK293T cells by standard procedures. Briefly, HEK293T cells were seeded at 1×10^6 cells per 10-cm plate and cotransfected the next day with 6 μg expressing plasmid with 4 μg of the packaging plasmid pCMV-dR8.91 and 2 μg envelope plasmid pMD2.G using Fugene6 reagent. The medium was changed after 24 h and 11 mg/ml BSA was added. Culture media were collected at 48 or 72 h after transfection and centrifuged at $330 \times g$ for 5 min to spin down cell debris. The resulting supernatant was used directly for infection of cells.

Proliferation and differentiation experiments

For proliferation assays, Runx2-null calvaria cells were plated at 10^5 cells per well in six-well plates and infected with lentivirus as described above. Cells were passed at d 3 after lentiviral infection and infected the next day with adenoviruses as described. After adenoviral infection for 24 h, cells were transferred to six-well plates at 10^5 cells per well. Growth curves were obtained by cell counting for 4 d.

For differentiation studies, mineralizing MC3T3-E1 cells or Runx2-null cells reconstituted with Runx2 expressed using an adenoviral vector were plated at a density of 0.4×10^6 cells per 100-mm plate in αMEM complemented with 30 mM penicillin-streptomycin, 100 mM L-glutamine, and 10% FBS (Hyclone). Cells were treated with 10 mM β-glycerophosphate and 25 μg/ml ascorbic acid in fresh media at d 4 after plating. The culture medium was supplemented with 10 mM β-glycerophosphate and 50 μg/ml ascorbic acid every other day for the remainder of the experiment.

Western blot analysis

For Western blotting, cell pellets were boiled in 100 μl direct lysis buffer [50 mM Tris-HCl (pH 6.8), 2% SDS, 10% glycerol, 12% urea, 25 μM MG132 (Calbiochem, EMD Biosciences, Inc., La Jolla, CA), 100 mM dithiothreitol, and 1× Complete protease inhibitors (Roche, Nutley, NJ)]. Aliquots (5 μl) of each lysate were separated using 10% SDS-PAGE and subjected to semi-wet transfer to polyvinylidene difluoride membranes (Millipore, Billerica, MA). PBS (1×)/0.1% Tween with 5% milk was used for 1 h to block nonspecific binding. Primary and secondary antibodies were used in a 1:2000 dilution for 1 h in PBS/0.1% Tween/1% milk. Signals were detected by chemiluminescence (PerkinElmer Western Lighting Chemiluminescence Reagent Plus; PerkinElmer, Waltham, MA). Cyp11a1 rabbit antiserum was a kind gift of Dr. Walter Miller (Department of Pediatrics, University of California at San Francisco) (76) and was incubated at 1:1000 dilution at 4 C overnight. Runx2-specific mouse monoclonal antibodies were the generous gift of Dr. Yoshi Ito (Institute for Molecular and Cellular Biology, Singapore). CDK2 rabbit polyclonal antibodies (M2) and β-actin goat polyclonal antibodies (C11) were purchased from Santa Cruz Biotechnology (Santa Cruz, CA).

qPCR analysis

Total RNA was extracted with Trizol reagent (Invitrogen) and purified on columns after deoxyribonucle-

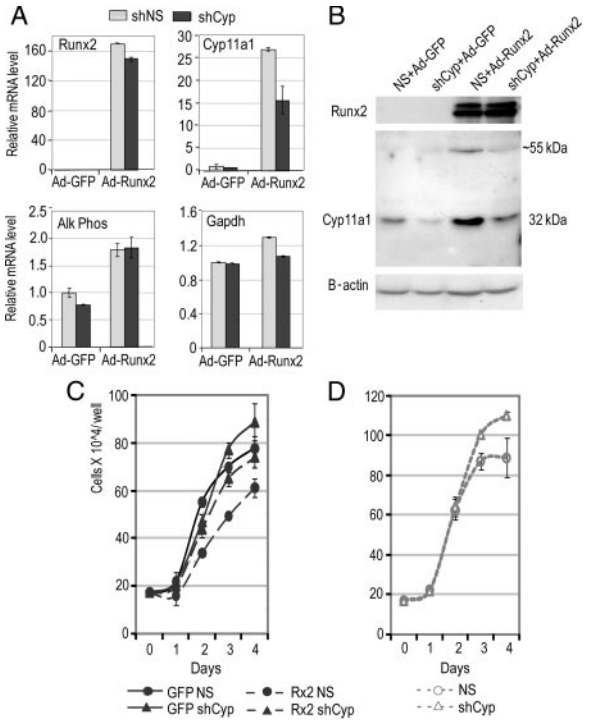

FIG. 10. shRNA-mediated knockdown of Cyp11a1 affects proliferation of osteoprogenitors. Cyp11a1 expression was knocked down with specific shRNAs delivered by lentiviral infection in Runx2-null mouse calvaria cells. Cells were passed 3 d later and infected with adenovirus expressing Runx2 (Ad-Runx2) or GFP-control virus (Ad-GFP) to induce Cyp11a1 gene expression in cells already treated with Cyp11a1 shRNA (shCyp) or nonspecific RNA control (NS). Cells were passed at identical density at 24 h after infection, and cell proliferation was monitored for the next 4 d. Runx2 overexpression and Cyp11a1 knockdown levels were monitored by qPCR (A) and Western blot analysis (B) at d 2 after adenoviral infection. C, Knockdown of Cyp11a1 after its induction by Runx2 modestly increases cell proliferation. Growth curves were obtained by cell counting. *Error bars* represent the SE among four different wells (from two experiments performed in duplicate). D Knockdown of endogenous Cyp11a1 increases cell proliferation. MC3T3 cells were infected with shRNA-lentivirus to knock down endogenous Cyp11a1 protein levels. Cells were replated after 3 d and counted for the next 4 d. *Error bars* represent SE among four different wells.

ase I treatment (RNA purification kit; Zymogen, Orange, CA). Total RNA aliquots (1 μg) were used for reverse transcription with random hexamers (Invitrogen). The resulting cDNA products were diluted from five to 75 times, and 5 μl was added in a 25-μl qPCR with Power SYBR Green PCR Master Mix (Applied Biosystems, Foster City, CA) for quantitation in an ABI Prism 7000 Sequence Detection System. PCR was performed using the following conditions: one cycle at 95 C for 10 min as the initial denaturation and 40 cycles of two-step reaction at 95 C for 15 sec (denaturation) and 60 C for 1 min (annealing and synthesis). The specific primers were used at a concentration of 0.5 pmol/μl in each reaction (Table 2).

Data normalization of samples from cell lines was established by qPCR with primers specific for rodent GAPDH and human 18S rRNA (Applied Biosystems). Primers to the mouse HPRT gene were used for normalization of qPCR data from different tissue samples. The same primers and conditions were used for representative semiquantitative RT-PCR except that only 25–30 cycles of synthesis were applied to avoid product saturation. Aliquots of the resulting product (5–20 μl) were visualized in 2% agarose gels by ethidium bromide staining.

In situ immunofluorescence

Immunofluorescence microscopy was performed according to standard procedures. Briefly, cells were grown on gelatin-coated coverslips and transfected or infected as described above, and 36 h after cells were fixed with 3.8% formaldehyde in PBS for 10 min and permeabilized with 0.25% Triton X-100 in PBS for 20 min. Nonspecific binding was blocked for 20 min with PBSA solution (PBS containing 0.5% BSA). The following primary antibodies were used for staining: rabbit antiserum to Cyp11a1 from Chemicon/Millipore (Chemicon International, Inc., Temecula. CA; catalog item 1294), at a dilution of 1:300 in PBSA at 37 C for 1 h and mouse monoclonal antibodies to Flag tag peptide from Sigma (clone M2, catalog item F1804) at a 1:1000 dilution at 37 C for 1 h. Secondary goat antimouse 488 (green) and goat antirabbit 568 (red) or goat antirabbit 488 (green) (Molecular Probes/Invitrogen, Eugene, OR) antibodies were used at a 1:800 dilution in PBSA for 1 h at 37 C. After the 4′,6-diamidino-2-phenylindole (DAPI) staining for 5 min for visualization of cell nuclei, coverslips were washed with PBS and mounted to the slides with Pro-long Gold mounting medium (Invitrogen). Double staining for Cyp11a1 and mitochondria was carried out using the Cyp11a1 antiserum and a mitochondrial marker (MitoTracker Red CMXRos from Invitrogen/Molecular Probes; catalog number M7512) according to protocols provided by the manufacturer. Fluorescence images were taken on an Axioplan 2 Carl Zeiss fluorescence microscope (Carl Zeiss, Thornwood, NY) with a Hamamatsu C4742-95 digital camera (Hamamatsu, Bridgewater, NJ). Digital images were acquired within the MetaMorph Imaging Series software environment (version 7.1.3) (Molecular Devices, Sunnyvale, CA).

Chromatin immunoprecipitation assay

Runx2-null calvaria cells were infected for 30 h with adenoviral vectors expressing Runx2 wild-type and IRES-GFP or GFP alone. Cells were then cross-linked with 1% formaldehyde for 10 min at room temperature followed by chromatin immunoprecipitations using Runx2 rabbit polyclonal antibodies M70 (Santa Cruz) as described previously (77). The primer pairs used for amplification of Runx2-bound fragments within the mouse Cyp11a1 promoter are listed in Table 2. Primers within the mouse GAPDH gene promoter were used as negative control.

Reporter gene assays

The −1.4-kb upstream sequence of the mouse Cyp11a1 gene (ENSMUSG 00000032323) was amplified with specific primers and cloned into the *Xho*I/*Hin*dIII sites of the pGL4 vector (Promega, Madison, WI). Subsequently, −0.3- and −0.2-kb promoter deletions were obtained by amplifying corresponding fragments, and the resulting PCR products were recloned into the *Xho*I-*Hin*dIII sites of pGL4. The sequences of specific primers that were used for promoter cloning are listed in Table 2. For reporter assays, Runx2-null mouse calvaria cells were seeded at 10^5 cells per well of a six-well plate. After 24 h, cells were infected with adenovirus expressing Runx2, its DNA-binding mutant, or GFP-expressing empty vector as described above. Cells were transfected 24 h after infection with each reporter construct (200 ng/well) and a renilla luciferase reporter vector (20 ng/well) (phRL-null; Promega) using Lipofectamine/Plus transfection reagents (Invitrogen). Luciferase activity was detected in cell lysates 24 h after transfection using the dual luciferase reporter system from Promega.

EMSA

ROS 17/2.8 cells were cultured to 90% of confluence and harvested in ice-cold PBS buffer by scraping. Cell pellets were lysed, and nuclear extracts prepared as previously described (78). Protein concentrations were determined by the Bradford method (Pierce Chemical Co., Rockford, IL). Sense and antisense oligonucleotides spanning a classical Runx2 motif (Rx2-C1) were end-labeled with [γ-^{32}P]ATP by use of T4 polynucleotide kinase (New England Biolabs, Beverly, MA) as documented in previous studies (78). Wild-type and mutant oligonucleotides (double stranded) were used as competitors. Nuclear protein extracts (5 μg) were incubated for 30 min at room temperature with 1 μg nonspecific competitor DNA poly (alternating dI-dC · dI-dC) (Pharmacia, Piscataway, NJ) and 80,000 cpm labeled oligonucleotides. Competition assays were performed by adding 100-fold molar

TABLE 2. Nucleotide sequences of the primers

Primers	Forward (5′–3′)	Reverse (5′–3′)
RT-PCR and qPCR primers		
Mouse Runx2	CGA CAG TCC CAA CTT CCT GT	CGG TAA CCA CAG TCC CAT CT
Mouse osteocalcin	CTG ACA AAG CCT TCA TGT CCA A	GCG CCG GAG TCT GTT CAC TA-3
Mouse Cyp11a1 exons 1/2	AGT GGC ACA CAG AAA ATC CA	TGG GGT CCA CGA TGT AAA CT
Mouse Cyp11a1 exons 2/3	CCA TTG GGG TCC TGT TTA AG	GGG GCA CGA AGT TCT TGA T
Mouse Cyp11a1 exons 3/4	TTC CTT TGA GTC CAT CAG CA	CAC TGG TGT GGA ACA TCT GG
Mouse Cyp11a1 exons 4/5	CTG CCT GGG ATG TGA TTT TC	CCC CAG GAG GCT ATA AAG GA
Mouse Cyp11a1 exons 5/6	CAG GCC AAC ATT ACC GAG AT	CGC AGC ATC TCC TGT ACC TT
Mouse Cyp11a1 exons 6/8	TTG GTT CCA CTC CTC AAA GC	GGC AAA GCT AGC CAC CTG TA
Mouse osteopontin	ACT CCA ATC GTC CCT ACA GTC G	TGA GGT CCT CAT CTG TGG CAT
Mouse Runx1	AGA TTC AAC GAC CTC AGG TTT GTC	CGG ATT TGT AAA GAC GGT GAT G
Mouse Cyp39a1	CAG TGT CCT GGA AGG TGG TT	GCT TTG GTA ATG GGT CCA GA-3
Mouse Cyp51	TCT CCA ATT CCA TTC CTT GG	GCC CAC CAT GGT AAA GCT AA-3
Mouse Dhcr7	TGG CTG CCC TAC CTC TAC AC	TAG TAA CCC ACG AGG CCA AG
Mouse Fdps	TCG TCA AGG TGC TGA CTG AG	CCG GTT GTA CTT GCC TCC TA
Mouse Lss	CGA CAT CAC TGC TCA GGA GA	TGG CAC AGG ACT TGT TGA AG
Mouse HPRT	CAG GCC AGA CTT TGT TGG AT	TTG CGC TCA TCT TAG GCT TT
Human osteocalcin	GGC AGC GAG GTA GTG AAG AG	CGA TAG GCC TCC TGA AAG C
Human CYP11A1	AGT CCA CCT TCA CCA TGT CC	GAG AAG GGC CAC ATC TTC AG
Human osteopontin	ACA CAT ATG ATG GCC GAG GT	ATG GCC TTG TAT GCA CCA TT
CHIP primers		
Cyp11a1 −1447	AGA CAC CCT GCT TTT CAT AAG G	CGG TTT GCT TGT TTT CCA TT
Cyp11a1 −1175	CCG TGA TTC CCT ATT AAA TCC A	TTC TAC CAC ATC CAG CTC AGG
Cyp11a1 −898	CTG AGG CAG GGG GAT CTT A	AAC CTG GAT CCT CTG GAA GAA
Cyp11a1 −250	GCC TCA TTT TCT TCC CAT GA	AGC TCC AGG CCT CTA ACC TC
Cyp11a1 +204	TCC TTC AAT GAG ATC CCT TCC	TCC TTC AAT GAG ATC CCT TCC
GAPDH	GTG CAT AGA GCC TCG GTA GG	CAG ATG AAC AGG GTG GGA AG-3
Primers used for cloning		
Cyp11a1 promoter, 1,400 bp	ATA AGG AAA ATA ATG TGT TA	AGG TTT GGG GCA GAG ACA CT
Cyp11a1 promoter, 300 bp	GAT CTC GAG CAT GAG CCA GGA GGT CTA	CGG AAG CTT AGT GTC TCT GCC CCA AAC
Cyp11a1 promoter, 200 bp	AAT CTC GAG AGG CCT GGA GCT GCC TG	CGG AAG CTT AGT GTC TCT GCC CCA AAC
Cyp11a1, 526 aa	CGC GAA TTC ATG CTG GCT AAA GGA CTT TC	GAT CTC GAG GCC TTC AGT TCA CAG TGT TG
Cyp11a1, 363 aa	CGC GAA TTC ATG GCG CCT GGA GCC ATC AA	CAT CTC GAG CAT GGG CCA CCT CCC CAT GT
EMSA oligos		
Rx2-C1	GTC ACC AAC CAC AGC ATC CTT TG	
Sp1-con	ATT CGA TCG GGG CGG GGC GAG C	
Rx2-C2	GGT CAC AAA CCA CAT GAT TCT GTC TC	
Rx2-C2mut	GGT CAC AA*g tCA* CAT GAT TCT GTC TC	
Cyp-1	GTG TTA GAA AGA CCA CAA ATT TTT CTT	
Cyp-2	TCT GAA GGA TAG TGG TCT TAG GGA CCC	
Cyp-3	CTG AGC TGG ATG TGG TAG AAC ATA GGT	
Cyp-4	TTT CTG TCA TAG TGG TGA ATG CAT ATA	
Cyp-5	GAG ATG GTT CAG TGG TTA AGA GCA CTG	

For EMSA oligos, only the sense strand is shown. Runx2 motifs are *underlined*; mutations are shown in *italics*.

excess of unlabeled oligonucleotides to the binding reaction. Protein-DNA complexes were separated in native 6% polyacrylamide gels and visualized by autoradiography of the dried gels.

The sequences of double-stranded cDNA oligonucleotides used in EMSA are listed in Table 2 (only the sense strand is shown, Runx2 motifs are *underlined*; mutations are shown in *italics*).

Acknowledgments

We thank Walter Miller (University of California, San Francisco, CA) critical reading of the manuscript and for the generous gift of Cyp11a1 antibody and Jim Neil (University of Glasgow, Scotland, UK) for sharing unpublished data on Runx target genes. We thank the members of our laboratories and especially Sadiq Hussain, Margaretha van der Deen, Anurag Gupta, Li-Jun Liu, Tripti Gaur, Tom Barthel, and Zhao-Yong Li for stimulating discussions, biological samples, and/or technical advice. We also thank Judy Rask for assistance with preparation of the manuscript.

Address all correspondence and requests for reprints to: Andre J. van Wijnen, Department of Cell Biology, 55 Lake Avenue North, Worcester, Massachusetts 01655-0106. E-mail: andre.vanwijnen@umassmed.edu.

This work was supported by National Institutes of Health Grants R01 AR49069 and R01 AR039588. The contents of this manuscript are solely the responsibility of the authors and do not necessarily represent the official views of the National Institutes of Health.

Disclosure Summary: The authors have nothing to disclose.

References

1. **Vanderschueren D, Gaytant J, Boonen S, Venken K** 2008 Androgens and bone. Curr Opin Endocrinol Diabetes Obes 15:250–254
2. **St-Arnaud R** 2008 The direct role of vitamin D on bone homeostasis. Arch Biochem Biophys 473:225–230
3. **Canalis E, Mazziotti G, Giustina A, Bilezikian JP** 2007 Glucocorticoid-induced osteoporosis: pathophysiology and therapy. Osteoporos Int 18:1319–1328

4. **Uitterlinden AG, Fang Y, Van Meurs JB, Pols HA, Van Leeuwen JP** 2004 Genetics and biology of vitamin D receptor polymorphisms. Gene 338:143–156
5. **Syed F, Khosla S** 2005 Mechanisms of sex steroid effects on bone. Biochem Biophys Res Commun 328:688–696
6. **Centrella M, Christakos S, McCarthy TL** 2004 Skeletal hormones and the C/EBP and Runx transcription factors: interactions that integrate and redefine gene expression. Gene 342:13–24
7. **van Driel M, Pols HA, van Leeuwen JP** 2004 Osteoblast differentiation and control by vitamin D and vitamin D metabolites. Curr Pharm Des 10:2535–2555
8. **Yanase T, Suzuki S, Goto K, Nomura M, Okabe T, Takayanagi R, Nawata H** 2003 Aromatase in bone: roles of vitamin D3 and androgens. J Steroid Biochem Mol Biol 86:393–397
9. **Boyan BD, Dean DD, Sylvia VL, Schwartz Z** 2003 Steroid hormone action in musculoskeletal cells involves membrane receptor and nuclear receptor mechanisms. Connect Tissue Res 44(Suppl 1):130–135
10. **Riggs BL, Khosla S, Melton 3rd LJ** 2002 Sex steroids and the construction and conservation of the adult skeleton. Endocr Rev 23:279–302
11. **Kato S, Takeyama K, Kitanaka S, Murayama A, Sekine K, Yoshizawa T** 1999 In vivo function of VDR in gene expression-VDR knock-out mice. J Steroid Biochem Mol Biol 69:247–251
12. **Kawano H, Sato T, Yamada T, Matsumoto T, Sekine K, Watanabe T, Nakamura T, Fukuda T, Yoshimura K, Yoshizawa T, Aihara K, Yamamoto Y, Nakamichi Y, Metzger D, Chambon P, Nakamura K, Kawaguchi H, Kato S** 2003 Suppressive function of androgen receptor in bone resorption. Proc Natl Acad Sci USA 100:9416–9421
13. **Smith EP, Boyd J, Frank GR, Takahashi H, Cohen RM, Specker B, Williams TC, Lubahn DB, Korach KS** 1994 Estrogen resistance caused by a mutation in the estrogen-receptor gene in a man. N Engl J Med 331:1056–1061
14. **Morishima A, Grumbach MM, Simpson ER, Fisher C, Qin K** 1995 Aromatase deficiency in male and female siblings caused by a novel mutation and the physiological role of estrogens. J Clin Endocrinol Metab 80:3689–3698
15. **Carani C, Qin K, Simoni M, Faustini-Fustini M, Serpente S, Boyd J, Korach KS, Simpson ER** 1997 Effect of testosterone and estradiol in a man with aromatase deficiency. N Engl J Med 337:91–95
16. **Migliaccio S, Brama M, Fornari R, Greco EA, Spera G, Malavolta N** 2007 Glucocorticoid-induced osteoporosis: an osteoblastic disease. Aging Clin Exp Res 19:5–10
17. **McClung MR** 2005 The relationship between bone mineral density and fracture risk. Curr Osteoporos Rep 3:57–63
18. **Sørensen MG, Henriksen K, Schaller S, Karsdal MA** 2007 Biochemical markers in preclinical models of osteoporosis. Biomarkers 12:266–286
19. **Rosen CJ** 2003 The cellular and clinical parameters of anabolic therapy for osteoporosis. Crit Rev Eukaryot Gene Expr 13:25–38
20. **Windahl SH, Andersson G, Gustafsson JA** 2002 Elucidation of estrogen receptor function in bone with the use of mouse models. Trends Endocrinol Metab 13:195–200
21. **Windahl SH, Lagerquist MK, Andersson N, Jochems C, Kallkopf A, Håkansson C, Inzunza J, Gustafsson JA, van der Saag PT, Carlsten H, Pettersson K, Ohlsson C** 2007 Identification of target cells for the genomic effects of estrogens in bone. Endocrinology 148:5688–5695
22. **McCarthy TL, Ji C, Shu H, Casinghino S, Crothers K, Rotwein P, Centrella M** 1997 17β-Estradiol potently suppresses cAMP-induced insulin-like growth factor-I gene activation in primary rat osteoblast cultures. J Biol Chem 272:18132–18139
23. **Ray A, Prefontaine KE, Ray P** 1994 Down-modulation of interleukin-6 gene expression by 17β-estradiol in the absence of high affinity DNA binding by the estrogen receptor. J Biol Chem 269:12940–12946
24. **Stein B, Yang MX** 1995 Repression of the interleukin-6 promoter by estrogen receptor is mediated by NF-κB and C/EBPβ. Mol Cell Biol 15:4971–4979
25. **Suda T, Nakamura I, Jimi E, Takahashi N** 1997 Regulation of osteoclast function. J Bone Miner Res 12:869–879
26. **Jilka RL, Weinstein RS, Parfitt AM, Manolagas SC** 2007 Quantifying osteoblast and osteocyte apoptosis: challenges and rewards. J Bone Miner Res 22:1492–1501
27. **McCarthy TL, Clough ME, Gundberg CM, Centrella M** 2008 Expression of an estrogen receptor agonist in differentiating osteoblast cultures. Proc Natl Acad Sci USA 105:7022–7027
28. **McCarthy TL, Hochberg RB, Labaree DC, Centrella M** 2007 3-Ketosteroid reductase activity and expression by fetal rat osteoblasts. J Biol Chem 282:34003–34012
29. **Centrella M, McCarthy TL, Chang WZ, Labaree DC, Hochberg RB** 2004 Estren (4-estren-3α,17β-diol) is a prohormone that regulates both androgenic and estrogenic transcriptional effects through the androgen receptor. Mol Endocrinol 18:1120–1130
30. **Sierra J, Villagra A, Paredes R, Cruzat F, Gutierrez S, Javed A, Arriagada G, Olate J, Imschenetzky M, van Wijnen AJ, Lian JB, Stein GS, Stein JL, Montecino M** 2003 Regulation of the bone-specific osteocalcin gene by p300 requires Runx2/Cbfa1 and the vitamin D3 receptor but not p300 intrinsic histone acetyltransferase activity. Mol Cell Biol 23:3339–3351
31. **McCarthy TL, Chang WZ, Liu Y, Centrella M** 2003 Runx2 integrates estrogen activity in osteoblasts. J Biol Chem 278:43121–43129
32. **Shen Q, Christakos S** 2005 The vitamin D receptor, Runx2, and the Notch signaling pathway cooperate in the transcriptional regulation of osteopontin. J Biol Chem 280:40589–40598
33. **Kitazawa S, Kajimoto K, Kondo T, Kitazawa R** 2003 Vitamin D3 supports osteoclastogenesis via functional vitamin D response element of human RANKL gene promoter. J Cell Biochem 89:771–777
34. **Jurutka PW, Bartik L, Whitfield GK, Mathern DR, Barthel TK, Gurevich M, Hsieh JC, Kaczmarska M, Haussler CA, Haussler MR** 2007 Vitamin D receptor: key roles in bone mineral pathophysiology, molecular mechanism of action, and novel nutritional ligands. J Bone Miner Res 22(Suppl 2):V2–V10
35. **van Wijnen AJ, Stein GS, Gergen JP, Groner Y, Hiebert SW, Ito Y, Liu P, Neil JC, Ohki M, Speck N** 2004 Nomenclature for Runt-related (RUNX) proteins. Oncogene 23:4209–4210
36. **Merriman HL, van Wijnen AJ, Hiebert S, Bidwell JP, Fey E, Lian J, Stein J, Stein GS** 1995 The tissue-specific nuclear matrix protein, NMP-2, is a member of the AML/CBF/PEBP2/runt domain transcription factor family: interactions with the osteocalcin gene promoter. Biochemistry 34:13125–13132
37. **Banerjee C, McCabe LR, Choi JY, Hiebert SW, Stein JL, Stein GS, Lian JB** 1997 Runt homology domain proteins in osteoblast differentiation: AML-3/CBFA1 is a major component of a bone specific complex. J Cell Biochem 66:1–8
38. **Ducy P, Zhang R, Geoffroy V, Ridall AL, Karsenty G** 1997 Osf2/Cbfa1: a transcriptional activator of osteoblast differentiation. Cell 89:747–754
39. **Drissi H, Pouliot A, Koolloos C, Stein JL, Lian JB, Stein GS, van Wijnen AJ** 2002 1,25(OH)$_2$Vitamin D3 suppresses the bone-related Runx2/Cbfa1 gene promoter. Exp Cell Res 274:323–333
40. **Viereck V, Siggelkow H, Tauber S, Raddatz D, Schutze N, Hüfner M** 2002 Differential regulation of Cbfa1/Runx2 and osteocalcin gene expression by vitamin-D3, dexamethasone, and local growth factors in primary human osteoblasts. J Cell Biochem 86:348–356
41. **Phillips JE, Gersbach CA, Wojtowicz AM, García AJ** 2006 Glucocorticoid-induced osteogenesis is negatively regulated by Runx2/Cbfa1 serine phosphorylation. J Cell Sci 119:581–591
42. **Kawate H, Wu Y, Ohnaka K, Takayanagi R** 2007 Mutual transactivational repression of Runx2 and the androgen receptor by an impairment of their normal compartmentalization. J Steroid Biochem Mol Biol 105:46–56
43. **Mikami Y, Takahashi T, Kato S, Takagi M** 2008 Dexamethasone promotes DMP1 mRNA expression by inhibiting negative regulation of Runx2 in multipotential mesenchymal progenitor, ROB-C26. Cell Biol Int 32:239–246
44. **Jüttner KV, Perry MJ** 2007 High-dose estrogen-induced osteogenesis is decreased in aged RUNX2$^{+/-}$ mice. Bone 41:25–32
45. **Young DW, Hassan MQ, Pratap J, Galindo M, Zaidi SK, Lee SH, Yang X, Xie R, Javed A, Underwood JM, Furcinitti P, Imbalzano AN, Penman S, Nickerson JA, Montecino MA, Lian JB, Stein JL, van Wijnen AJ, Stein GS** 2007 Mitotic occupancy and lineage-specific transcriptional control of rRNA genes by Runx2. Nature 445:442–446
46. **Young DW, Hassan MQ, Yang XQ, Galindo M, Javed A, Zaidi SK, Furcinitti P, Lapointe D, Montecino M, Lian JB, Stein JL, van Wijnen AJ, Stein GS** 2007 Mitotic retention of gene expression patterns by the cell fate determining transcription factor Runx2. Proc Natl Acad Sci USA 104:3189–3194
47. **Pratap J, Galindo M, Zaidi SK, Vradii D, Bhat BM, Robinson JA, Choi JY, Komori T, Stein JL, Lian JB, Stein GS, van Wijnen AJ** 2003 Cell growth regulatory role of Runx2 during proliferative expansion of pre-osteoblasts. Cancer Res 63:5357–5362
48. **Galindo M, Pratap J, Young DW, Hovhannisyan H, Im HJ, Choi JY, Lian JB, Stein JL, Stein GS, van Wijnen AJ** 2005 The bone-specific expression of RUNX2 oscillates during the cell cycle to support a G1 related anti-proliferative function in osteoblasts. J Biol Chem 280:20274–20285
49. **Zaidi SK, Pande S, Pratap J, Gaur T, Grigoriu S, Ali SA, Stein JL, Lian JB, van Wijnen AJ, Stein GS** 2007 Runx2 deficiency and defective subnuclear targeting bypass senescence to promote immortalization and tumorigenic potential. Proc Natl Acad Sci USA 104:19861–19866
50. **Kilbey A, Blyth K, Wotton S, Terry A, Jenkins A, Bell M, Hanlon L, Cameron ER, Neil JC** 2007 Runx2 disruption promotes immortalization and confers resistance to oncogene-induced senescence in primary murine fibroblasts. Cancer Res 67:11263–11271

51. **Teplyuk NM, Galindo M, Teplyuk VI, Pratap J, Young DW, Lapointe D, Javed A, Stein JL, Lian JB, Stein GS, van Wijnen AJ** 2008 Runx2 regulates G-protein coupled signaling pathways to control growth of osteoblast progenitors. J Biol Chem 283:27585–27597
52. **Blyth K, Vaillant F, Hanlon L, Mackay N, Bell M, Jenkins A, Neil JC, Cameron ER** 2006 Runx2 and MYC collaborate in lymphoma development by suppressing apoptotic and growth arrest pathways in vivo. Cancer Res 66:2195–2201
53. **Blyth K, Cameron ER, Neil JC** 2005 The runx genes: gain or loss of function in cancer. Nat Rev Cancer 5:376–387
54. **Galindo M, Kahler RA, Teplyuk NM, Stein JL, Lian JB, Stein GS, Westendorf JJ, van Wijnen AJ** 2007 Cell cycle related modulations in Runx2 protein levels are independent of lymphocyte enhancer-binding factor 1 (Lef1) in proliferating osteoblasts. J Mol Histol 38:501–506
55. **Wotton S, Terry A, Kilbey A, Jenkins A, Herzyk P, Cameron E, Neil JC** 2008 Gene array analysis reveals a common Runx transcriptional programme controlling cell adhesion and survival. Oncogene 27:5856–5866
56. **Otto F, Lübbert M, Stock M** 2003 Upstream and downstream targets of RUNX proteins. J Cell Biochem 89:9–18
57. **Stock M, Schfer H, Fliegauf M, Otto F** 2004 Identification of novel genes of the bone-specific transcription factor Runx2. J Bone Miner Res 19:959–972
58. **Gaikwad JS, Cavender A, D'Souza RN** 2001 Identification of tooth-specific downstream targets of Runx2. Gene 279:91–97
59. **Bae JS, Gutierrez S, Narla R, Pratap J, Devados R, van Wijnen AJ, Stein JL, Stein GS, Lian JB, Javed A** 2007 Reconstitution of Runx2/Cbfa1-null cells identifies a requirement for BMP2 signaling through a Runx2 functional domain during osteoblast differentiation. J Cell Biochem 100:434–449
60. **Storbeck KH, Swart P, Swart AC** 2007 Cytochrome P450 side-chain cleavage: insights gained from homology modeling. Mol Cell Endocrinol 265–266: 65–70
61. **Pikuleva IA** 2006 Cytochrome P450s and cholesterol homeostasis. Pharmacol Ther 112:761–773
62. **Jo M, Curry Jr TE** 2006 Luteinizing hormone-induced RUNX1 regulates the expression of genes in granulosa cells of rat periovulatory follicles. Mol Endocrinol 20:2156–2172
63. **Shimada M, Hernandez-Gonzalez I, Gonzalez-Robayna I, Richards JS** 2006 Paracrine and autocrine regulation of epidermal growth factor-like factors in cumulus oocyte complexes and granulosa cells: key roles for prostaglandin synthase 2 and progesterone receptor. Mol Endocrinol 20:1352–1365
64. **Miller WL** 1995 Mitochondrial specificity of the early steps in steroidogenesis. J Steroid Biochem Mol Biol 55:607–616
65. **Lambeth JD, Stevens VL** 1984 Cytochrome P-450scc: enzymology, and the regulation of intramitochondrial cholesterol delivery to the enzyme. Endocr Res 10:283–309
66. **Nelson DR, Zeldin DC, Hoffman SM, Maltais LJ, Wain HM, Nebert DW** 2004 Comparison of cytochrome P450 (CYP) genes from the mouse and human genomes, including nomenclature recommendations for genes, pseudogenes and alternative-splice variants. Pharmacogenetics 14:1–18
67. **Paredes R, Arriagada G, Cruzat F, Villagra A, Olate J, Zaidi K, van Wijnen A, Lian JB, Stein GS, Stein JL, Montecino M** 2004 Bone-specific transcription factor Runx2 interacts with the 1α,25-dihydroxyvitamin D3 receptor to up-regulate rat osteocalcin gene expression in osteoblastic cells. Mol Cell Biol 24:8847–8861
68. **Lambertini E, Penolazzi L, Tavanti E, Schincaglia GP, Zennaro M, Gambari R, Piva R** 2007 Human estrogen receptor α gene is a target of Runx2 transcription factor in osteoblasts. Exp Cell Res 313:1548–1560
69. **Viccica G, Vignali E, Marcocci C** 2007 Role of the cholesterol biosynthetic pathway in osteoblastic differentiation. J Endocrinol Invest 30:8–12
70. **Jeong JH, Jin JS, Kim HN, Kang SM, Liu JC, Lengner CJ, Otto F, Mundlos S, Stein JL, van Wijnen AJ, Lian JB, Stein GS, Choi JY** 2008 Expression of Runx2 transcription factor in non-skeletal tissues, sperm and brain. J Cell Physiol 217:511–517
71. **Hu MC, Hsu NC, El Hadj NB, Pai CI, Chu HP, Wang CK, Chung BC** 2002 Steroid deficiency syndromes in mice with targeted disruption of Cyp11a1. Mol Endocrinol 16:1943–1950
72. **Tuckey RC, Li W, Zjawiony JK, Zmijewski MA, Nguyen MN, Sweatman T, Miller D, Slominski A** 2008 Pathways and products for the metabolism of vitamin D3 by cytochrome P450scc. FEBS J 275:2585–2596
73. **Zbytek B, Janjetovic Z, Tuckey RC, Zmijewski MA, Sweatman TW, Jones E, Nguyen MN, Slominski AT** 2008 20-Hydroxyvitamin D3, a product of vitamin D3 hydroxylation by cytochrome P450scc, stimulates keratinocyte differentiation. J Invest Dermatol 128:2271–2280
74. **Slominski A, Semak I, Wortsman J, Zjawiony J, Li W, Zbytek B, Tuckey RC** 2006 An alternative pathway of vitamin D metabolism: cytochrome P450scc (CYP11A1)-mediated conversion to 20-hydroxyvitamin D2 and 17,20-dihydroxyvitamin D2. FEBS J 273:2891–2901
75. **Prince M, Banerjee C, Javed A, Green J, Lian JB, Stein GS, Bodine PV, Komm BS** 2001 Expression and regulation of Runx2/Cbfa1 and osteoblast phenotypic markers during the growth and differentiation of human osteoblasts. J Cell Biochem 80:424–440
76. **Black SM, Szklarz GD, Harikrishna JA, Lin D, Wolf CR, Miller WL** 1993 Regulation of proteins in the cholesterol side-chain cleavage system in JEG-3 and Y-1 cells. Endocrinology 132:539–545
77. **Hovhannisyan H, Cho B, Mitra P, Montecino M, Stein GS, Van Wijnen AJ, Stein JL** 2003 Maintenance of open chromatin and selective genomic occupancy at the cell-cycle-regulated histone H4 promoter during differentiation of HL-60 promyelocytic leukemia cells. Mol Cell Biol 23:1460–1469
78. **Hassan MQ, Javed A, Morasso MI, Karlin J, Montecino M, van Wijnen AJ, Stein GS, Stein JL, Lian JB** 2004 Dlx3 transcriptional regulation of osteoblast differentiation: temporal recruitment of Msx2, Dlx3, and Dlx5 homeodomain proteins to chromatin of the osteocalcin gene. Mol Cell Biol 24:9248–9261
79. **Zhang Y, Hassan MQ, Li ZY, Stein JL, Lian JB, van Wijnen AJ, Stein GS** 2008 Intricate gene regulatory networks of helix-loop-helix (HLH) proteins support regulation of bone-tissue related genes during osteoblast differentiation. J Cell Biochem 105:487–496